# Sensorless Vector Control of Induction Motor Using A Novel Reduced-Order Extended Luenberger Observer

Jooho Song, Kyo-Beum Lee, Joong-Ho Song, Ick Choy, and Kwang-Bae Kim
Intelligent System Control Research Center, Korea Institute of Science and Technology
39-1 Hawolgok-dong, Sungbuk-gu, Seoul 136-791, Korea
Tel: +82-2-958-5756, Fax: +82-2-958-5749, E-mail: jhsong@amadeus.kist.re.kr

***Abstract*-A synthesis method of the reduced-order extended Luenberger observer (ROELO) and its design procedure for a nonlinear dynamic system are presented. This paper proposes a method to reduce the order of the observer and to select the observer gain matrix. The main features of the proposed observer are discussed and compared with the characteristics of the other observers. The proposed algorithm is applied for high-performance induction motor drives without a speed sensor. The simulation results show that the proposed ROELO provides both the rotor flux and rotor speed estimation with good transient and steady state performance**

## I. INTRODUCTION

Vector control drive is a prevailing control principle for induction motors. Correct estimation of the rotor flux is one of the most critical steps of major problems occurred in the implementation of vector-controlled induction motor drive. The rotor flux can be obtained in some ways if the speed is directly measured. In some applications, however, the elimination of speed sensors is desirable as they tend to reduce system reliability when working in hostile environments. Several types of observers have been applied for speed sensorless drive systems: adaptive observer [1, 2] and extended Luenberger observer [1, 3, 4]. Adaptive observer consists of a linear observer for the rotor flux estimation and an adaptive scheme for the rotor speed estimation. An expected problem in a sequential estimation, in which the speed estimator follows the rotor flux estimator, is such that the speed estimation error may be amplified by the action of the state estimator [1]. In the sensorless control scheme using the extended Luenberger observer, the error amplification can be avoided since the rotor flux and the rotor speed are estimated simultaneously. However, since the dimension of the extended Luenberger observer is higher than that of adaptive observer, computational requirements may be more demanding. Hence, the reduced-order extended Luenberger observer is preferable in application.

This paper describes the characteristics of reduced-order extended Luenberger observer. There are two methods to reduce the dimension of the observer; one is based on the matrix transformation, and the other is based on the known-states elimination. The first method proposed by Orlowska-Kowalska [3] and Du [4] is easy of design, however it has a problem of poor transient response characteristics. Therefore, this paper proposes a design procedure to reduce the order using the second method and a method to select the observer gain matrix. This paper shows a comprehensively comparative study among adaptive observer (AO), the first method of the extended Luenberger observer (ROELO1), and the second method of the extended Luenberger observer (ROELO2).

## II. MOTOR MODEL AND EXTENDED LUENBERGER OBSERVER

### A. Motor Model

In general, the rate of change of the system parameters is slower than that of the state variables in the electromechanical dynamic system. Since the induction motor speed can be considered as a slowly time-varying variable, comparing with electrical state variables, the motor speed can be regarded as a system parameter that is assumed to keep a zero time-derivative in the discrete implementation. Hence, the motor speed can be expressed as (1). Note that the arguments of time are omitted in the following equations for their simplification.

$$\dot{\omega}_r = 0 \tag{1}$$

As a result, the augmented motor equation for deriving the ROELO algorithm consists of the basic electrical equations and the motor speed equation of (1). The augmented nonlinear model of an indirect vector-controlled induction motor in rotor flux reference frame can be expressed like the following equations:

$$\begin{aligned} \dot{x} &= f(x) + Bu \\ y &= Cx \end{aligned} \tag{2}$$

where

$$x = [i_{qs}^e \quad i_{ds}^e \quad \varphi_{qr}^e \quad \varphi_{dr}^e \quad \omega_r]^T$$
$$y = [i_{qs}^e \quad i_{ds}^e]^T \qquad u = [v_{qs}^e \quad v_{ds}^e]^T \tag{3}$$
$$f[x] =$$

$$\begin{bmatrix} -\left(\frac{R_s}{\sigma L_s} + \frac{1-\sigma}{\sigma}\rho\right) i_{qs}^e - (\omega_r + \omega_{sl}) i_{ds}^e + X\rho\varphi_{qr}^e - X\omega_r\varphi_{dr}^e \\ (\omega_r + \omega_{sl}) i_{qs}^e - \left(\frac{R_s}{\sigma L_s} + \frac{1-\sigma}{\sigma}\rho\right) i_{ds}^e + X\omega_r\varphi_{qr}^e + X\rho\varphi_{qr}^e \\ L_m\rho i_{qs}^e - \rho\varphi_{qr}^e + \omega_{sl}\varphi_{dr}^e \\ L_m\rho i_{ds}^e + \omega_{sl}\varphi_{qr}^e - \rho\varphi_{dr}^e \\ 0 \end{bmatrix} \tag{4}$$

$$B = \begin{bmatrix} \frac{L_r}{L_s L_r - L_m^2} & 0 \\ 0 & \frac{L_r}{L_s L_r - L_m^2} \\ 0 & 0 \\ 0 & 0 \\ 0 & 0 \end{bmatrix} \quad C = \begin{bmatrix} 1 & 0 & 0 & 0 & 0 \\ 0 & 1 & 0 & 0 & 0 \end{bmatrix} \tag{5}$$

0-7803-6401-5/00/$10.00 © 2000 IEEE

$$\sigma = 1 - \frac{L_m^2}{L_s L_r} \quad X = \frac{L_m}{\sigma L_s L_r} \quad \rho = \frac{1}{T_r} \quad \omega_{sl} = \rho \frac{i_{qs}^{e*}}{i_{ds}^{e*}} \quad (6)$$

where $i_{qs}^{e*}$ and $i_{ds}^{e*}$ are current commands in vector control.

*B. Extended Luenberger Observer*

Since this model equation is nonlinear, a linearization is required. Equation (2) can be linearized by Jacobian approximation.

$$\begin{aligned} \dot{x} &= f(x) + Bu \approx f(\bar{x}) + \left.\frac{\partial f(x)}{\partial x}\right|_{x=\bar{x}} (x - \bar{x}) + Bu \\ &= \left.\frac{\partial f(x)}{\partial x}\right|_{x=\bar{x}} x + Bu + f(\bar{x}) - \left.\frac{\partial f(x)}{\partial x}\right|_{x=\bar{x}} \bar{x} \\ &= A(\bar{x})x + Bu + g(\bar{x}) \end{aligned} \quad (7)$$

where $\bar{x}$ is reference trajectory which is usually chosen as $\hat{x}(t - \Delta t)$, an estimate of the state vector at time $(t - \Delta t)$, and

$$A(\bar{x}) = \begin{bmatrix} -\frac{R_s}{\sigma L_s} - \frac{1-\sigma}{\sigma}\rho & -\bar{\omega}_r - \omega_{sl} & X\rho & -X\bar{\omega}_r & -\bar{i}_{ds}^e - X\bar{\varphi}_{dr}^e \\ \bar{\omega}_r + \omega_{sl} & -\frac{R_s}{\sigma L_s} - \frac{1-\sigma}{\sigma}\rho & X\bar{\omega}_r & X\rho & \bar{i}_{qs}^e + X\bar{\varphi}_{qr}^e \\ L_m\rho & 0 & -\rho & -\omega_{sl} & 0 \\ 0 & L_m\rho & \omega_{sl} & -\rho & 0 \\ 0 & 0 & 0 & 0 & 0 \end{bmatrix} \quad (8)$$

$$g(\bar{x}) = \begin{bmatrix} (\bar{i}_{ds}^e + X\bar{\varphi}_{dr}^e)\bar{\omega}_r \\ -(\bar{i}_{qs}^e + X\bar{\varphi}_{qr}^e)\bar{\omega}_r \\ 0 \\ 0 \\ 0 \end{bmatrix} \quad (9)$$

It is noted that the linearized equation (7) is linear time-invariant within one sampling interval. Therefore, the conventional theory of the linear Luenberger observer can be used to formulate an observer at every sampling interval and to estimate the unknown states at the next sampling time. The full-order extended Luenberger observer can be structured as (10) based on the linearized model equation.

$$\begin{aligned} \dot{\hat{x}}(t) &= A(\bar{x})\hat{x}(t) + Bu(t) + G[y(t) - C\hat{x}(t)] + g(\bar{x}) \\ &= (A(\bar{x}) - GC)\hat{x}(t) + Bu(t) + Gy(t) + g(\bar{x}) \end{aligned} \quad (10)$$

## III. Reduced-Order Observer Theory

The full-order extended Luenberger observer is in fifth order. Hence, the calculation of gain matrix is very heavy and difficult. To make calculation of gain matrix easier, reduced-ordered model is preferred. Since two states, *d-q* stator current, are known, the dimension of the augmented model can be reduced to third order. There are two dimension-reducing methods. They are described in detail. It is of interest to estimate only the unmeasured augmented states by using a reduced-order extended Luenberger observer.

*A. Method 1* [3, 4, 5]

This method is based on the matrix transformation. For reducing the $(n+p)$th order observer to the $p$th order, temporary state vector, $z$ in the $p$th order, is defined as follows;

$$z = Tx = \begin{bmatrix} T_1 & T_2 \end{bmatrix} \begin{bmatrix} x_n \\ \hat{x}_p \end{bmatrix} \quad (11)$$

where, $x_n$ is the known state vector, $x_p$ is the unknown state vector and $T$ is transformation matrix including $T_1 \in \Re^{p \times n}$ and $T_2 \in \Re^{p \times p}$. Note that $T_2$ must be invertible.

Using this transformation, the full-order observer of (10) is reduced to (12), the first type reduced-order extended Luenberger observer (ROELO1).

$$\dot{z} = Fz + Gy + TBu + Tg \quad (12)$$

where $F$ is the system matrix of the reduced-order observer, which is chosen according to the desired pole location. The gain matrix $G$ is obtained by the following Lyapunov equation:

$$TA - FT = GC. \quad (13)$$

The original states are obtained by inverse transform of (11).

$$\hat{x}_p = T_2^{-1}(z - T_1 x_n) \quad (14)$$

This observer can be implemented if the following conditions are satisfied [5].

(1) $F$ and $A$ have no common eigenvalue.
(2) $(F, G)$ is controllable and $(A, C)$ is observable.

This method has an advantage that a designer can locate the poles of the observer arbitrarily, whereas a disadvantage to solve Lyapunov equation with high computation burden remains.

*B. Method 2 (Proposed Method)*

This order-reducing method is based on cancellation of the known states. The system can be partitioned as

$$\begin{aligned} \begin{bmatrix} \dot{x}_n \\ \dot{x}_p \end{bmatrix} &= \begin{bmatrix} A_{11} & A_{12} \\ A_{21} & A_{22} \end{bmatrix} \begin{bmatrix} x_n \\ x_p \end{bmatrix} + \begin{bmatrix} B_1 \\ 0 \end{bmatrix} u + \begin{bmatrix} g_1 \\ g_2 \end{bmatrix} \\ y &= \begin{bmatrix} I & 0 \end{bmatrix} \begin{bmatrix} x_n \\ x_p \end{bmatrix} = x_n \end{aligned} \quad (15)$$

This can be rearranged as follows:

$$\begin{aligned} \dot{y} &= \dot{x}_n = A_{11}x_n + A_{12}x_p + B_1 u + g_1 \\ \dot{x}_p &= A_{21}x_n + A_{22}x_p + g_2 = A_{21}y + A_{22}x_p + g_2 \end{aligned} \quad (16)$$

Let

$$\begin{aligned}\bar{u} &= A_{21}y + g \\ w &= A_{12}x_p = \dot{y} - A_{11}y - B_1u - g_1\end{aligned}, \tag{17}$$

then reduced-order system equation is obtained as

$$\begin{aligned}\dot{x}_p &= A_{22}x_p + \bar{u} \\ w &= A_{12}x_p\end{aligned} \tag{18}$$

An observer for (18) is constructed as follows:

$$\begin{aligned}\dot{\hat{x}}_p &= A_{22}\hat{x}_p + G(w - A_{12}\hat{x}_p) + \bar{u} \\ &= (A_{22} - GA_{12})\hat{x}_p + Gw + \bar{u} \\ &= (A_{22} - GA_{12})\hat{x}_p + G(\dot{y} - A_{11}y - B_1u - g_1) + A_{21}y + g_2\end{aligned} \tag{19}$$

This equation involves the derivative of $y$ that may take some bad effects such as noise amplification on estimation. This can be eliminated by defining temporary state vector, $z$.

$$z = \hat{x}_p - Gy \tag{20}$$

By substituting (20) into (19), equation (19) yields (21), the second type reduced-order extended Luenberger observer (ROELO2).

$$\begin{aligned}\dot{z} &= (A_{22} - GA_{12})(z + Gy) + (A_{21} - GA_{11})y - G(B_1u + g_1) + g_2 \\ &= (A_{22} - GA_{12})z + [(A_{22} - GA_{12})G + (A_{21} - GA_{11})]y \\ &\quad -G(B_1u + g_1) + g_2\end{aligned} \tag{21}$$

The original states are reconstructed by the following equation obtained from (20).

$$\hat{x}_p = z + Gy \tag{22}$$

This method has an advantage that it requires simple calculation relative to the method 1. However it has a disadvantage that the free design of observer pole location is somewhat difficult. A method to overcome this sustaining problem is described in the following section.

## IV. Observer Gain Selection

For the gain selection of the ROELO2, this paper proposes the pole-decoupling method. From (18) and (19), the error dynamic equation is obtained as (23). Note that $A_{12}$ is updated with the estimated rotor flux and the estimated rotor speed.

$$\begin{aligned}\dot{e} = (A_{22} - GA_{12})e &= \left( \begin{bmatrix} -\rho & -\omega_{sl} & 0 \\ \omega_{sl} & -\rho & 0 \\ 0 & 0 & 0 \end{bmatrix} \right. \\ &\quad \left. - \begin{bmatrix} g_{11} & g_{12} \\ g_{21} & g_{22} \\ g_{31} & g_{32} \end{bmatrix} \begin{bmatrix} X\rho & -X\hat{\omega}_r & -i_{ds}^e - X\hat{\varphi}_{dr}^e \\ X\hat{\omega}_r & X\rho & i_{qs}^e + X\hat{\varphi}_{qr}^e \end{bmatrix} \right) e \\ &= \begin{bmatrix} -\rho - g_{11}X\rho - g_{12}X\hat{\omega}_r & -\omega_{sl} + g_{11}X\hat{\omega}_r - g_{12}X\rho \\ \omega_{sl} - g_{21}X\rho - g_{22}X\hat{\omega}_r & -\rho + g_{21}X\hat{\omega}_r - g_{22}X\rho \\ -g_{31}X\rho - g_{32}X\hat{\omega}_r & g_{31}X\hat{\omega}_r - g_{32}X\rho \end{bmatrix} \\ &\quad \begin{matrix} g_{11}(i_{ds}^e + X\hat{\varphi}_{dr}^e) - g_{12}(i_{qs}^e + X\hat{\varphi}_{qr}^e) \\ g_{21}(i_{ds}^e + X\hat{\varphi}_{dr}^e) - g_{22}(i_{qs}^e + X\hat{\varphi}_{qr}^e) \\ g_{31}(i_{ds}^e + X\hat{\varphi}_{dr}^e) - g_{32}(i_{qs}^e + X\hat{\varphi}_{qr}^e) \end{matrix} \Bigg] e \\ &= \begin{bmatrix} m_{11} & m_{12} & m_{13} \\ m_{21} & m_{22} & m_{23} \\ m_{31} & m_{32} & m_{33} \end{bmatrix} e\end{aligned} \tag{23}$$

To decouple the poles of the rotor flux estimation from that of the rotor speed estimation, $m_{13}$ and $m_{23}$ in (23) are set to be zero. Then, the pole of the rotor flux estimation is determined by the 2x2 leading principal minor, $\begin{bmatrix} m_{11} & m_{12} \\ m_{21} & m_{22} \end{bmatrix}$, and the pole of rotor speed estimation by $m_{33}$.

$$\begin{aligned}m_{13} &= g_{11}(i_{ds}^e + X\hat{\varphi}_{dr}^e) - g_{12}(i_{qs}^e + X\hat{\varphi}_{qr}^e) = 0 \\ m_{23} &= g_{21}(i_{ds}^e + X\hat{\varphi}_{dr}^e) - g_{22}(i_{qs}^e + X\hat{\varphi}_{qr}^e) = 0\end{aligned} \tag{24}$$

These can be rearranged with respected to $g_{11}$ and $g_{21}$. $g_{12}$ and $g_{22}$ are tuned for good performance.

$$g_{11} = g_{12}\frac{i_{qs}^e + X\hat{\varphi}_{qr}^e}{i_{ds}^e + X\hat{\varphi}_{dr}^e} \qquad g_{21} = g_{22}\frac{i_{qs}^e + X\hat{\varphi}_{qr}^e}{i_{ds}^e + X\hat{\varphi}_{dr}^e} \tag{25}$$

For stability, the eigenvalues of error equation must have negative real part. Let

$$Y = \frac{i_{qs}^e + X\hat{\varphi}_{qr}^e}{i_{ds}^e + X\hat{\varphi}_{dr}^e}, \tag{26}$$

then (23) yields (27) by substituting (25) and (26) into (23).

$$\dot{e} = \begin{bmatrix} -\rho - n_1 g_{12} & -\omega_{sl} + n_2 g_{12} \\ \omega_{sl} - n_1 g_{22} & -\rho + n_2 g_{22} \\ -g_{31}X\rho - g_{32}X\hat{\omega}_r & g_{31}X\hat{\omega}_r - g_{32}X\rho \end{bmatrix} \begin{matrix} 0 \\ 0 \\ g_{31}(i_{ds}^e + X\hat{\varphi}_{dr}^e) - g_{32}(i_{qs}^e + X\hat{\varphi}_{qr}^e) \end{matrix} \Bigg] e \tag{27}$$

where

$$\begin{aligned}n_1 &= X(Y\rho + \hat{\omega}_r) \\ n_2 &= X(Y\hat{\omega}_r - \rho)\end{aligned}. \tag{28}$$

First, the characteristic equation of the 2x2 leading principal minor of error matrix in (27) is

$$s^2+(2\rho+n_1g_{12}-n_2g_{22})s+\rho^2+(n_1g_{12}-n_2g_{22})\rho +\omega_{sl}^2-(n_2g_{12}+n_1g_{22})\omega_{sl}=0 \quad (29)$$

Assume that the roots are complex, $a \pm jb$. Then the characteristic equation becomes

$$(s-a+jb)(s-a-jb)=s^2-2as+a^2+b^2=0. \quad (30)$$

Since $a$ must be smaller than the original system pole $-\rho$ for stability and fast estimation, the coefficient of $s$, $-2a$ must be bigger than $2\rho$. Equating like coefficients of (29) and (30), following inequality is obtained:

$$n_1g_{12}-n_2g_{22}>0. \quad (31)$$

Assume that the roots are real, $a$ and $b$. Then the characteristic equation becomes

$$(s-a)(s-b)=s^2-(a+b)s+ab=0. \quad (32)$$

Since $a$ and $b$ must be smaller than $-\rho$ for stability and fast estimation, the coefficient of $s$, $-(a+b)$ must be bigger than $2\rho$, and $ab$ bigger than $\rho^2$. Equating like coefficients of (29) and (32), following inequality is obtained:

$$\begin{aligned} &n_1g_{12}-n_2g_{22}>0 \\ &(n_1g_{12}-n_2g_{22})\rho+\omega_{sl}^2-(n_2g_{12}+n_1g_{22})\omega_{sl}>0 \end{aligned} \quad (33)$$

Since (31) appears in (33), $g_{11}$ and $g_{21}$ should be selected to satisfy the inequality condition of (33). As a result, the two poles of three are determined to have negative real part.

Secondly, the remaining pole is determined by $m_{33}$. For stability, it must be negative.

$$m_{33}=g_{31}(i_{ds}^e+X\hat{\varphi}_{dr}^e)-g_{32}(i_{qs}^e+X\hat{\varphi}_{qr}^e)<0 \quad (34)$$

Remembering that the elements, $g_{11}$ and $g_{21}$ of the observer gain matrix are determined in (25), the other gain elements, $g_{12}$, $g_{22}$, $g_{31}$ and $g_{32}$, should be selected under the inequality conditions of (33) and (34). A helpful tuning method to satisfy them described as follows: $g_{12}$ and $g_{22}$ are set to be negative and positive respectively and to vary in proportion to the rotor speed. $g_{31}$ is set negative constant, and $g_{32}$ to vary in positive proportion to the speed.

As an example, the flows of poles related with the rotor flux estimation and the rotor speed estimation are shown in Fig. 1, where the root locus is plotted by using the simulation results as the motor speed varies from zero to high speed.

## V. Simulation

The specification of the induction motor used for simulation is shown in Table I, and the sampling time of each control loop is in Table II. All simulations using ROELO1, ROELO2, and adaptive observer are performed under the same conditions.

Fig. 2 shows the overall control block diagram of sensorless vector-controlled induction motor drive system using the ROELO2. Since the observer is located in the feedback path of the speed and rotor flux loops, the observer

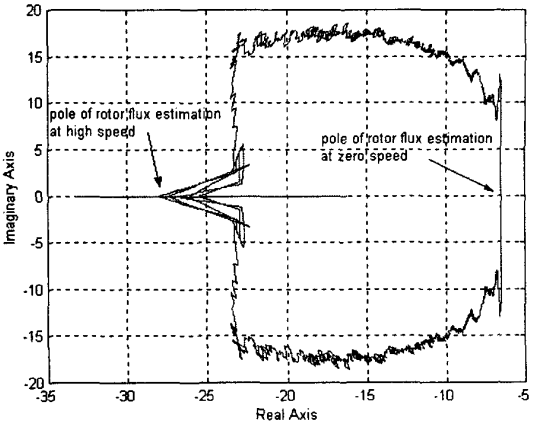


(a)

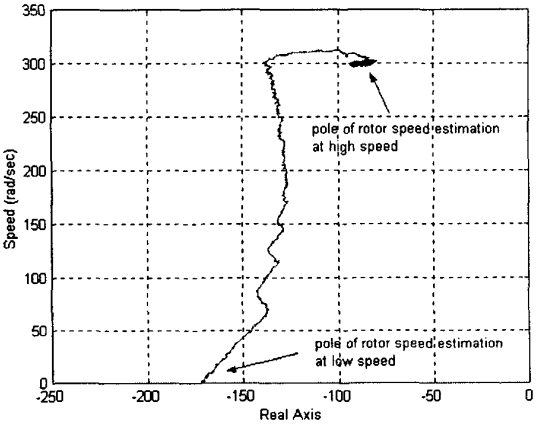


(b)

Fig. 1. The flow of the pole location along to rotor speed; (a) the poles of rotor flux estimation; (b) the pole of rotor speed estimation

TABLE I
Induction motor specification

| | |
|---|---|
| Rated Power | 10 hp |
| Rated Voltage | 320 $V_{LL}$ |
| Rated Speed | 1740 rpm |
| Number of Poles | 4 |
| Stator Resistance ($R_s$) | 0.1695 Ω |
| Rotor Resistance ($R_r$) | 0.161 Ω |
| Mutual Inductance ($L_m$) | 22.77 mH |
| Stator Leakage Inductance ($L_{sl}$) | 1.2 mH |
| Rotor Leakage Inductance ($L_{rl}$) | 1.79 mH |

TABLE II
Sampling frequency of each control loop

| | |
|---|---|
| Inverter PWM | 540 Hz |
| Speed Loop | 2.16 kHz |
| Current Loop | 2.16 kHz |
| Observer Loop | 2.16 kHz |

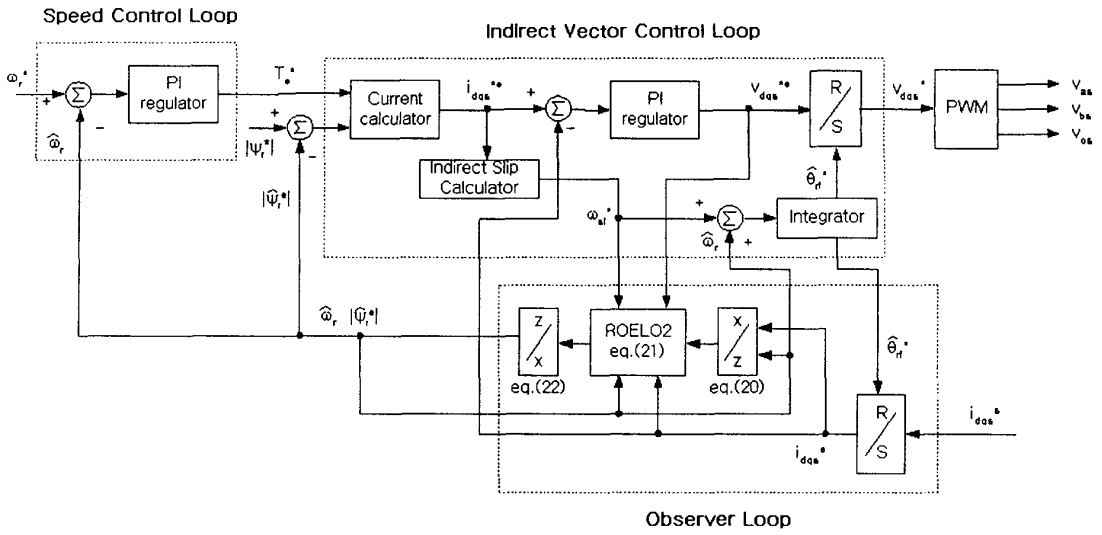


Fig. 2. Closed-loop control block diagram using the ROELO2

behavior takes a deep effect on the system performance. It is important that the estimator generates accurate estimation in the steady state to achieve the required system accuracy. It is also critical that the dynamics of the estimator are sufficiently fast to meet the transient performance requirements of a high-performance vector-controlled drive.

*A. ROELO2*

Fig. 3 shows the performance of ROELO2 when the speed reference varies in the forward and reverse rotation. In the wide speed range, estimation and control of the speed and the flux show good performance. It is noted from the Fig. 3 that the estimation error around the zero-crossing of the speed becomes consdering large.

The performance of the step load applied is shown in Fig. 4. The low-speed performace without load and with load are shown in Fig. 5 and 6, respectively. In this case, the motor speed is controlled at 1% rated speed.

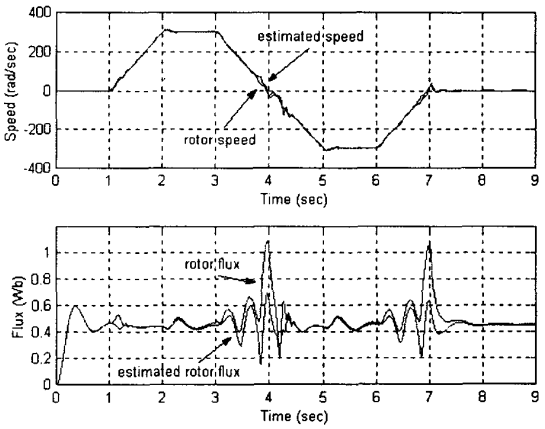


Fig. 3. Sensorless control performance using ROELO2

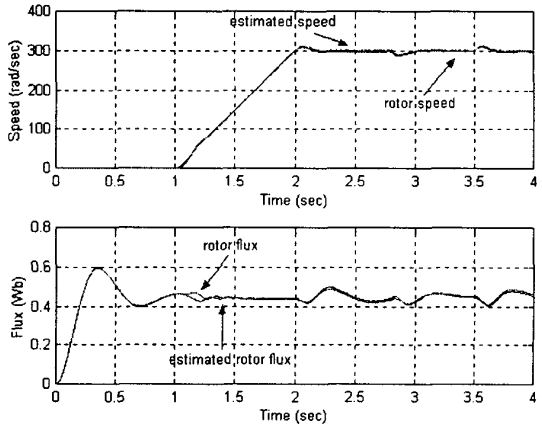


Fig. 4. Simulation results using ROELO2 at high speed when 30Nm load is applied for 0.7sec.

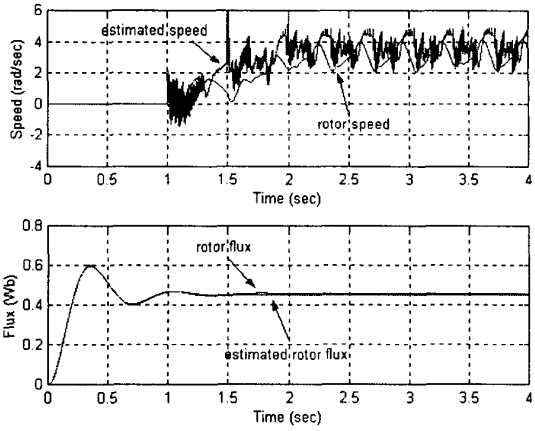


Fig. 5. Simulation results using ROELO2 at low speed when no load is applied.

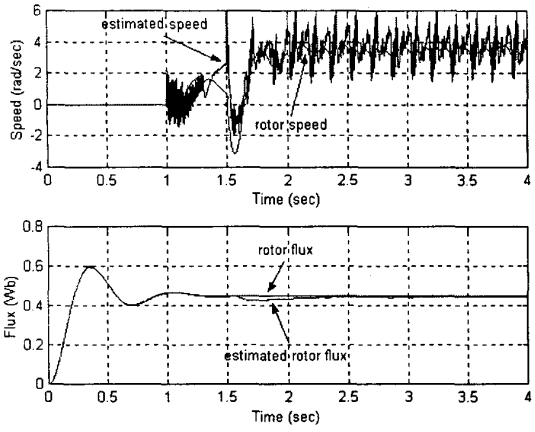


Fig. 6. Simulation results using ROELO2 at low speed when 10Nm load is applied from 1.5sec.

### *B. Comparison with Other Observers*

It can be said from the simulation results in the previous section that ROELO2 provides proper state estimation for sensorless vertor control of induction motor drive. In this section, some comparative investigation are done among ROELO1, ROELO2, and adaptive observer.

Fig. 7 shows the ramp-up responses from zero to high speed. Note that Fig. 7(a) and (c) show only the beginning part of each response, and Fig. 7(b) shows response in longer time span. When adaptive observer is used, the estimated speed oscillates as illustrated in Fig, 7(a). It is caused from sequential connection of the flux estimator and the rotor speed estimator as described in introduction. Fig. 7(b) shows the response when ROELO1. For simulation of ROELO1, the poles are located at -100, -100 and -10, and transformation matrix $T$ is set as (35).

$$T = \begin{bmatrix} t_{11} & t_{12} & 1 & 0 & t_{15} \\ t_{21} & t_{22} & 0 & 1 & t_{25} \\ t_{31} & t_{32} & 1 & 1 & t_{35} \end{bmatrix} \qquad (35)$$

In this case, the speed during ramp-up is not estimated well as reported in [4]. Since $T_2^{-1}$ in (14) is chattering around zero during initial time and ramp-up time for the low rotor speed or the low slip frequency, the reconstructed states may not follow the real values. On the contrary, the ramp-up speed estimation of ROELO2 shows good response as shown in Fig. 7(c).

When AO and ROELO1 are used, the sensorless control performances at the low speed and without load are shown in Fig. 8. It is seen from these figures that the speed estimation using AO does not work and ROELO1 supports no-load low-speed control. However, the estimated value of ROELO1 is often abruptly changed and the speed oscillation is occurred largely. When using ROELO2, low speed response without load is better as shown in Fig. 5.

When the step load is applied during ramp-up transient, adaptive observer and ROELO2 support sensorless control performance as shown in Fig. 9. ROELO1 response diverges. Fig. 9(b) (the same figure as upper part of Fig. 6) shows more smoothed speed response than Fig. 9(a).

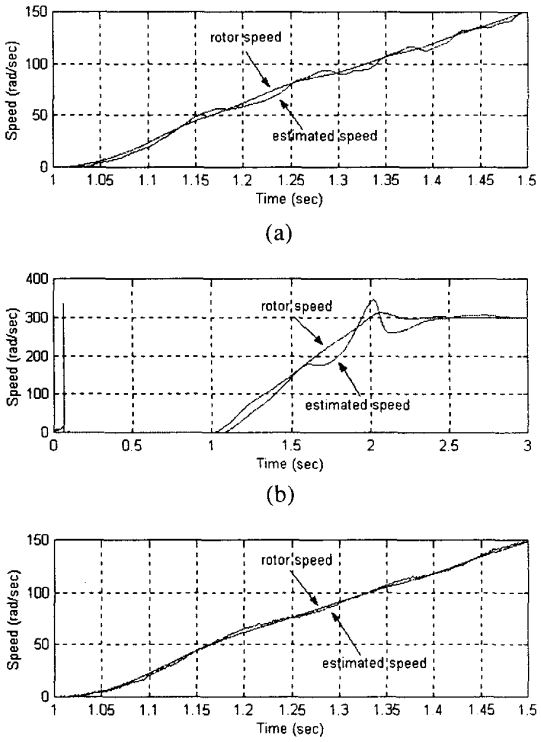


Fig. 7. Ramp-up speed response from zero to high speed: (a) when using AO; (b) when using ROELO1 (c) when using ROELO2

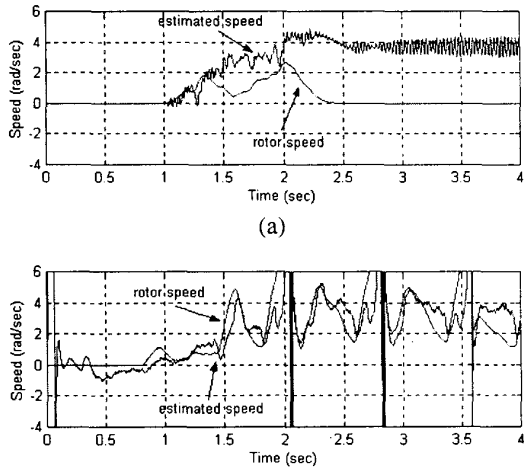


Fig. 8. Simulation results at low speed without load; (a) using AO; (b) using ROELO1

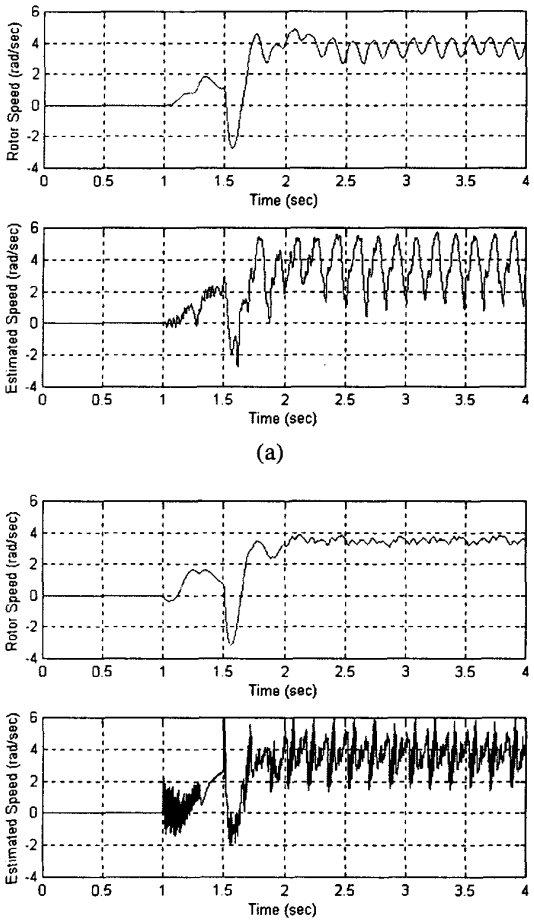


Fig. 9. Simulation results at low speed when 10Nm load is applied after 1.5sec.; (a) when using AO; (b) when using ROELO2

## VI. Conclusion

The detailed design procedure for the reduced-order extended Luenberger observer has been presented. Especially, the order-reducing method based on cancellation of the known states and the pole-decoupling method for the observer gain selection have been proposed and described in detail. The main features of the ROELO2 have been discussed and compared with the characteristics of the adaptive observer and ROELO1.

The ROELO2 has been successfully applied to induction motor sensorless drive system. It can be said from the simulation results that the estimation of rotor speed and rotor flux has been done satisfactorily. ROELO2 has better characteristics than other observers have.

## References

[1] P. Vas, *Sensorless Vector Control and Direct Torque Control*, Oxford, New York, 1998

[2] H. Kubota, K. Matsuse, "Speed Sensorless Field-Oriented Control of Induction Motor with Rotor Resistance Adaptation," *IEEE Trans. Ind. Appl., Vol. 30, No. 5*, pp.224-229, Sep./Oct., 1994

[3] T. Orlowska-Kowalska, "Application of extended Luenberger observer for flux and rotor time-constant estimation in induction motor drives," *IEE Proc., Vol. 136, Pt.D, No. 6*, pp.324-330, Nov., 1989

[4] T. Du, M. A. Brdys, "Shaft Speed, Load Torque and Rotor Flux Estimation of Induction Motor Drive Using an Extended Luenberger Observer," *Proceedings of 6th International Conference on Electrical Machines and Drives. IEE Conf. Pub. 376*, pp.179-184, 1993

[5] C.-T. Chen, *Linear System Theory and Design*, 3rd ed., Oxford, New York, 1999